

See discussions, stats, and author profiles for this publication at: <https://www.researchgate.net/publication/7505489>

Surface-Enhanced Raman Scattering on Nanoshells with Tunable Surface Plasmon Resonance

ARTICLE *in* LANGMUIR · DECEMBER 2005

Impact Factor: 4.46 · DOI: 10.1021/la051645l · Source: PubMed

CITATIONS

72

READS

56

4 AUTHORS, INCLUDING:



Ramón A Alvarez-Puebla

Catalan Institution for Research and Advanc...

141 PUBLICATIONS 5,108 CITATIONS

SEE PROFILE



Gholam-Abbas Nazri

Wayne State University

98 PUBLICATIONS 1,799 CITATIONS

SEE PROFILE



Ricardo F Aroca

University of Windsor

314 PUBLICATIONS 6,824 CITATIONS

SEE PROFILE

Surface-Enhanced Raman Scattering on Nanoshells with Tunable Surface Plasmon Resonance

Ramon A. Alvarez-Puebla, Daniel J. Ross, G.-Abbas Nazri, and Ricardo F. Aroca*

Materials and Surface Science Group, Faculty of Sciences, University of Windsor, Windsor, Ontario, Canada N9B 3P4

Received June 18, 2005. In Final Form: August 24, 2005

Fabrication, characterization, and optical enhancement applications of bimetallic AgAu nanoparticles and nanoshells are reported. Nanoparticles with tunable surface plasmon resonances are synthesized at room temperature and characterized by transmission electron microscopy, X-ray photoelectron spectroscopy, and photon correlation spectroscopy. The collective electron oscillation of the nanoparticles shows a controllable tunability in the 400–990 nm spectral range, in agreement with plasmon absorption calculated using Mie theory, providing an optimum substrate for surface plasmon-assisted enhanced spectroscopy. Surface-enhanced Raman scattering experiments show that the average enhancement factor obtained with nanoshells could be higher than those obtained with silver sols.

Introduction

The collective oscillation of the electrons in metal nanoparticles (surface plasmon resonance-SPR) has been, and is, the object of intense multidisciplinary research with a wide scope of applications.^{1–3} The intimate connection between the SPR and surface-enhanced spectroscopy has been experimentally demonstrated using surface-enhanced Raman excitation spectra (SERES).⁴ It was confirmed that the SERES spectra are correlated, both spatially and spectrally, with the corresponding surface plasmon resonance spectra of the nanoparticle arrays in full compliance with the electromagnetic mechanism.^{5,6} In heterogeneous SERS substrates such as colloidal aggregates of films, it has been found that the plasmon-enhanced near field interparticle coupling provides field confinement and highly enhanced fields (hot spots) that have been used in single molecule detection.^{7,8} The exact correlation between the hot spots (places with giant field enhancement) and SPR is under scrutiny.⁹ In general, in the surface plasmon-assisted enhanced spectroscopy, there is a need to optimize the correlation between the surface plasmon resonance and the excitation laser line. SERS practitioners have at their disposal a large variety of laser lines, where the most commonly used in dispersive Raman instrumentation are in the 400–830 nm spectral region. The FT-SERS uses the 1064 nm line. The most common silver and gold sols used in SERS, offer a narrow distribution of surface plasmons, ranging from 390 to 440

nm for silver and 500 to 560 nm with gold. By controlling both particle size and shape, a modest tunability of the plasmon absorption can be achieved.^{2,3} There are also reports on bimetallic alloys with plasmon absorption covering a wide range from 400 to 550 nm.^{10,11} However, Halas et al.^{12,13} have reported a surface plasmon shift of 600–1200 nm in gold nanoshells, and Sun and Xia¹⁴ have reported an interval of plasmons between 425 and 1030 nm, and very recently Liang et al.¹⁵ have reported the making of uniform gold hollow nanospheres with tunable interior-cavity sizes with SPR in the 526 to 628 nm. Therefore, nanoshells, i.e., hollow metal nanoparticles, provide a substrate that can be made with tunable surface plasmon resonance, giving rise to highly desirable nanoparticles with many potential applications at a reduced cost.

Most of the nanoshell fabrication methods use templates of silica or polymers, coating the surface of these templates with the desired metal, and removing the templates by calcinations at elevated temperature, or by dissolving the cores with the appropriate solvent. An elegant chemical approach uses a metallic colloidal particle, the core metal having smaller reduction potential than the metal selected for the shell. This method, was initially proposed by Sun and Xia^{15,16} and in this procedure, the authors recommend heating the reaction to obtain smooth single-crystal surfaces via Oswald ripening.¹⁷ The fabrication of these shells with smooth walls may have a broad range of applications, including electronics, information storage or biological and chemical sensing. However, for catalytic applications and surface-enhanced spectroscopy particles with ultra-rough surface, nanostructures that simulate aggregates of smooth particles are preferable. Recently, Jackson and Halas¹⁸ have also examined the SERS effect

* To whom correspondence should be addressed. E-mail: rarocal@cogeco.ca.

(1) Kreibig, U.; Vollmer, M. *Optical Properties of Metal Clusters*; Springer-Verlag: Berlin, 1995; Vol. 25.

(2) Kelly, K. L.; Coronado, E.; Zhao, L. L.; Schatz, G. C. *J. Phys. Chem. B* **2003**, *107*, 668–677.

(3) Link, S.; El-Sayed, M. A. *Int. Rev. Phys. Chem.* **2000**, *19*, 409–453.

(4) McFarland, A. D.; Young, M. A.; Dieringer, J. A.; Van Duyne, R. P. *J. Phys. Chem. B* **2005**, *109*, 11279–11285.

(5) Moskovits, M. *Rev. Mod. Phys.* **1985**, *57*, 783–826.

(6) Schatz, G. C.; Van Duyne, R. P. In *Handbook of Vibrational Spectroscopy*; Chalmers, J. M., Griffiths, P. R., Eds.; John Wiley & Sons, Ltd.: Chichester, U.K., 2002; Vol. 1, pp 759–774.

(7) Lu, H. P. *J. Phys. Condens. Mater.* **2005**, *17*, R333–R355.

(8) Stockman, M. I.; Faleev, S. V.; Bergman, D. J. *Phys. Rev. Lett.* **2001**, *87*, 167401/167401–167401/167404.

(9) Etchegoin, P.; Cohen, L. F.; Hartigan, H.; Brown, R. J. C.; Milton, M. J. T.; Gallop, J. C. *J. Chem. Phys.* **2003**, *119*, 5281–5289.

(10) Chen, D.-H.; Chen, C.-J. *J. Mat. Chem.* **2002**, *12*, 1557–1562.

(11) Rodriguez-Gonzalez, B.; Sanchez-Iglesias, A.; Giersig, M.; Liz-Marzan Luis, M. *Faraday Discuss.* **2004**, *125*, 133–144; discussion 195–219.

(12) West, J. L.; Halas, N. J. *Ann. Rev. Biomed. Eng.* **2003**, *5*, 285–292.

(13) Halas, N. *Opt. Photonics News* **2002**, *13*, 26–30.

(14) Sun, Y.; Xia, Y. *J. Am. Chem. Soc.* **2004**, *126*, 3892–3901.

(15) Sun, Y.; Mayers, B. T.; Xia, Y. *Nano Lett.* **2002**, *2*, 481–485.

(16) Sun, Y.; Xia, Y. *Anal. Chem.* **2002**, *74*, 5297–5305.

(17) Roosen, A. R.; Carter, W. C. *Phys. A* **1998**, *261*, 232–247.

(18) Jackson, J. B.; Halas, N. J. *Proc. Natl. Acad. Sci. U.S.A.* **2004**, *101*, 17930–17935.

using nanoshells and concluded that enhancement was mainly assisted by individual nanoparticles (rather than aggregates). Here, we report the results of the synthesis of nanoparticles and nanoshells under thermodynamic conditions that favor the formation of these rough, heterogeneous nanostructures. The bimetallic nature of the nanoshells could also help the selective adsorption and retention of analytes. For instance, both Ag and Au are class B elements in accordance with Pearson theory;^{19,20} however, Ag readily adsorb N-containing groups, whereas gold preferentially adsorb S-containing groups.

Experimental Methods

The production of the bimetallic nanoshells was based on the method proposed by Xia's group.^{15,16} Briefly, 100 mL of Ag nanoparticles were prepared by using the citrate reduction method.²¹ The colloidal suspension was then diluted to 1 L with Milli-Q water (Millipore) in order to decrease its tendency toward aggregation and titrated with KAuCl_4 10^{-3} M solution under strong agitation at room temperature with 1 h intervals of between additions (from 5 to 40 mL at 5 mL intervals). Samples of 25 mL were stored after each addition and kept under agitation at room temperature for 24 h before the characterization.

UV-visible extinction spectra (300–1100 nm) of the nanoshell suspensions were recorded with a Varian Cary 50 UV-visible spectrophotometer. X-ray photoelectron spectroscopy (Physical Electronics PHI-5500) was carried out on samples prepared by casting 20 aliquots of 10 μL (total volume of 200 μL) of the different colloidal suspensions on a Ti Foil. Zeta potential values were determined by injecting 10 mL aliquots of the colloidal solutions into a Malvern Zetasizer HS3000 photon correlation spectrometer with an applied voltage of 100 V and a 5-cm quartz cell. To ensure reproducibility, two separate samples were studied, and three measurements were co-added for each one.²² Hydrodynamic size was determined in the same instrument by introducing 5 mL of the colloidal suspensions into a 1 cm path length quartz cell and employing dynamic light scattering at an angle of 90°. TEM analysis was performed with a Philips CM12 operating at 120 kV.²³ Theoretical computation of extinction cross-sections for nanoshells was carried out using the Mie formalism for concentric spheres from Bohren and Huffman,²⁴ on Maple 9.

Samples for SERS were prepared by adding 10 μL of 10^{-3} M of 2-naphthalenethiol (Aldrich) to 1 mL of colloidal suspension. Average SERS spectra were collected with a Renishaw Invia system, equipped with CCD detector and a Leica microscope. The spectrographs use 1800 g/mm gratings with additional band-pass filter optics. Excitation lines of 514.5, 633, and 785 nm were used. Spectra were collected in Renishaw's extended collection mode, by co-adding three scans with accumulation times of 10 s.

Results and Discussion

Silver citrate colloids exhibit different spherical-like morphologies with a broad particle size distribution. Particle sizes of ca. 50 nm are found in the transmission electron microscopy (TEM) image (Figure 1A). As synthesized, silver citrate colloids exhibited a greenish yellow color with a surface resonance plasmon at 442 nm. To obtain the bimetallic colloids and shells, the silver citrate colloids were titrated at room temperature with different volumes of 10^{-3} M gold solution (5–40 mL) of KAuCl_4 (Aldrich). The first addition of gold (5 mL) gives a red-

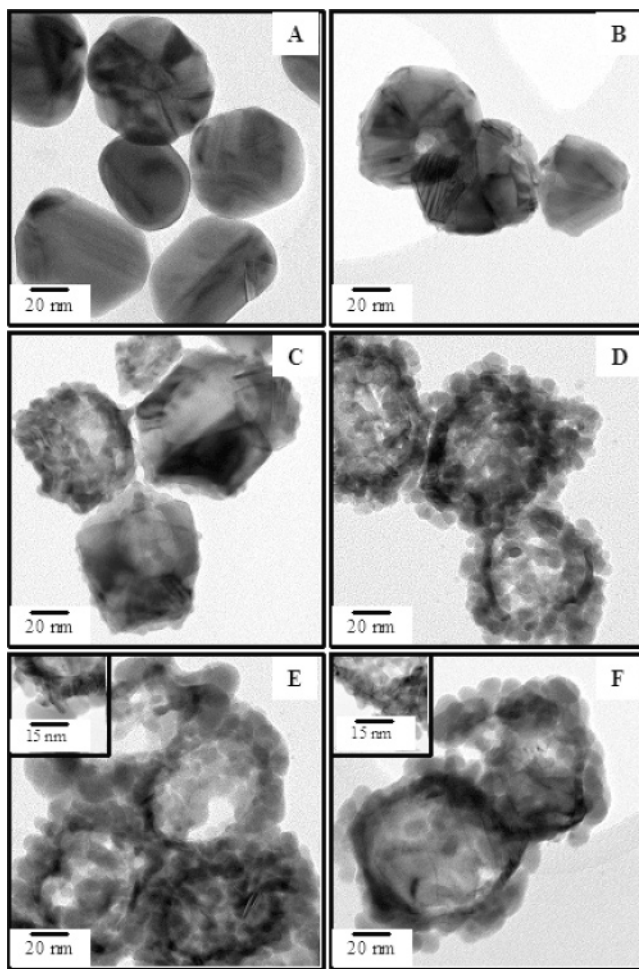


Figure 1. Transmission electron microscopy images of (A) silver citrate colloids, and silver citrate colloids treated with different volumes of 10^{-3} M gold solution: (B) 5 mL, (C) 10 mL, (D) 15 mL, (E) 20 mL, and (F) 25 mL. The insets in E and F show high-resolution images of the nanoshell walls.

colored solution with a broad surface plasmon with a maximum at 489 nm (Figure 2B, second spectrum maximum from the left). At the beginning of the hollow formation process (Figure 1b), minor changes in the size and shape of the nanoparticles are revealed by the HRTEM images. From this point on, the reaction leads to a hollow interior and the formation of a rough exterior wall in accordance with Oswald ripening^{15,25} (Figure 1c–d). The growth of the hollow interior is characterized by a dramatic red shift in the surface plasmon from 533 to 949 nm as can be seen in Figure 2. This shift in the surface plasmon resonance is a peculiar property of nanoshells, a property that cannot be achieved with solid nanoparticles of the same metal.^{25,26}

Mie theory calculations for concentric silver nanoshell spheres^{24,27} support the observations, and the red shift in the maximum of the plasmon resonance is found to be proportional to the size of the radius of the inner hollow sphere as can be seen in Figure 2B. The results presented are in full agreement with Mie calculations on similar systems.²⁸ The model particles were given an outer radius of 25 nm, corresponding to observed sizes from Figure 1C,

(19) Pearson, R. G. *Science* **1966**, *151*, 172–177.

(20) Pearson, R. G. *J. Am. Chem. Soc.* **1963**, *85*, 3533–3539.

(21) Creighton, J. A.; Blatchford, C. G.; Albrecht, M. G. *J. Chem. Soc., Faraday Trans. 2* **1979**, *75*, 790–798.

(22) Alvarez-Puebla, R. A.; Arceo, E.; Goulet, P. J. G.; Garrido, J. J.; Aroca, R. F. *J. Phys. Chem. B* **2005**, *109*, 3787–3792.

(23) Yao, Z.; Braidy, N.; Botton, G. A.; Adronov, A. *J. Am. Chem. Soc.* **2003**, *125*, 16015–16024.

(24) Bohren, C. F.; Huffman, D. R. *Absorption and Scattering of Light by Small Particles*; Wiley-Interscience: New York, 1983.

(25) Schelm, S.; Smith, G. B. *J. Phys. Chem. B* **2005**, *109*, 1689–1694.

(26) Averitt, R. D.; Sarkar, D.; Halas, N. J. *Phys. Rev. Lett.* **1997**, *78*, 4217–4220.

(27) Aragon, S. R.; Elwenspoek, M. *J. Chem. Phys.* **1982**, *77*, 3406.

(28) Sun, Y.; Xia, Y. *Analyst* **2003**, *128*, 686–691.

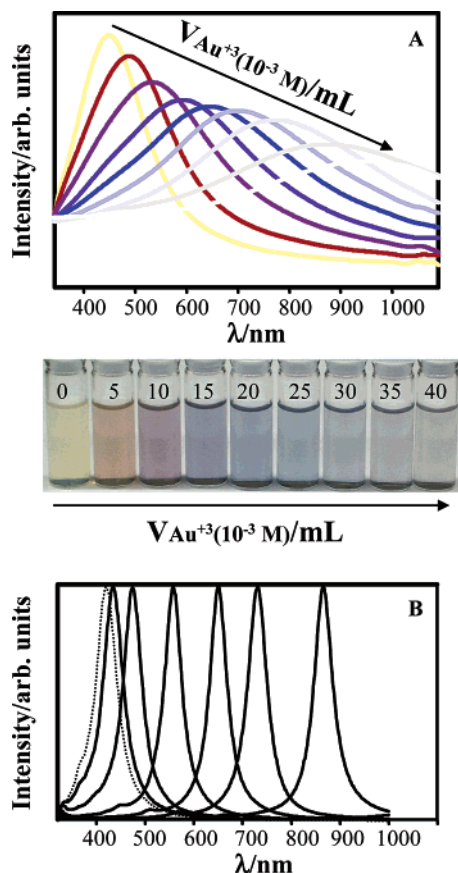


Figure 2. (A) Surface plasmon absorption of the prepared colloids as a function of the volume of gold added. Appearance of the colloidal suspensions. (B) Mie calculations results for solid ($r = 25$ nm) Ag sphere and (from left to right) nanoshells with inner radii is 10, 15, 19, 21, and 23 nm; core and external media are aqueous.

and both the external and core material is assumed to be water ($n = 1.33$). The use of silver is reasonable as an illustration of the plasmonic tunability, and similar results are obtained with gold. The calculated homogeneous bandwidth of the nanoshell's plasmon is on average close to 50 nm, whereas the observed inhomogeneous bandwidth for the experimental ensemble ranges from 198 nm for silver citrate colloids and 243 nm for the first bimetallic colloids ($V_{Au} = 5$ mL) to 348 nm for the last bimetallic nanoshell ($V_{Au} = 40$ mL).

Notably, all of the observed plasmon spectra show only one broad peak (Figure 2A), which may indicate the formation of a gold/silver alloy, which is possible given their close match in crystalline structure and lattice constants. The bimetallic nature of the prepared nanoparticles is supported by the results of X-ray photoelectron spectroscopy (XPS) of samples cast onto Ti foil. The nanoparticles prepared as indicated above, show both Ag 3d and Au 4f peaks with high intensity (Figure 3A,B). In full agreement with the chemistry, the peaks due to silver (Figure 3A) decrease, whereas those due to gold (Figure 3B) increase as the volume of gold used in the titration increases. The percentage of Au within the X-ray penetration depth on the shell surface was quantified by Au 4f and Ag 3d areas and is shown in Figure 3C as a function of the volume of Au^{3+} added. This percentage ranges from 6.3% with a volume of gold added of 5 mL to 54.5% when the added volume was 40 mL. It is possible to add more gold to the colloidal suspension in order to obtain pure gold nanoshells; however, that was not the aim of the present work.

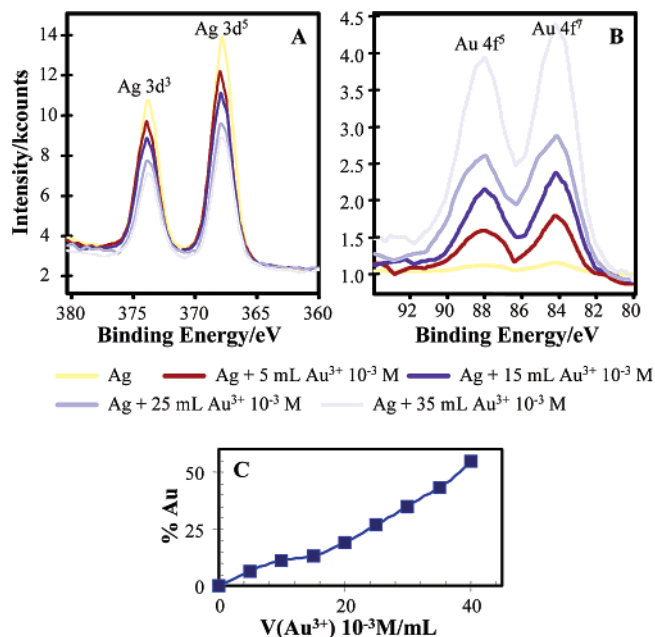


Figure 3. X-ray photoelectron spectroscopy of the colloids as a function of the volume of gold added. (A) Silver 3d bands, (B) gold 4f bands, and (C) percentage of gold on the shell as a function of the volume of gold added.

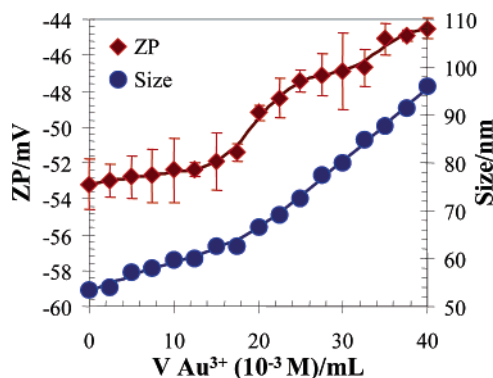


Figure 4. Zeta potential and hydrodynamic size of the colloids as a function of the volume of gold added.

Figure 4 shows the variation of both the zeta potential and hydrodynamic size with the volume of gold added. The zeta potential (ξ) shows a consistent tendency to increase as the gold is added. Therefore, the ξ value ranges from -53.2 mV for silver colloids, which is in agreement with the literature values,^{22,29} to -44.5 mV when the volume of gold added in this experiment was 40 mL. This range of values is very important because it indicates that the colloidal suspension is stable during the entire titration range in compliance with Derjaguin–Verwey–Landau–Overbeek (DLVO) theory.³⁰ The latter is a critical factor to achieve good “average SERS” signal, since colloidal suspensions with ξ values near -20 mV tend to aggregate and flocculate (and the aggregation increases even further when an analyte is added), leading to a damping of the SERS signal, due to removal of active SERS colloidal nanoparticles. Figure 4 shows a consistent increase in the hydrodynamic size of the colloids, due to the gold accumulation on the outer surface of the shell, with each volume of gold added. In this case the hydrodynamic size

(29) Faulds, K.; Littleford, R. E.; Graham, D.; Dent, G.; Smith, W. E. *Anal. Chem.* **2004**, 76, 592–598.

(30) Shaw, D. J. *Introduction to colloid and surface chemistry*; Butterworth: London, 1980.

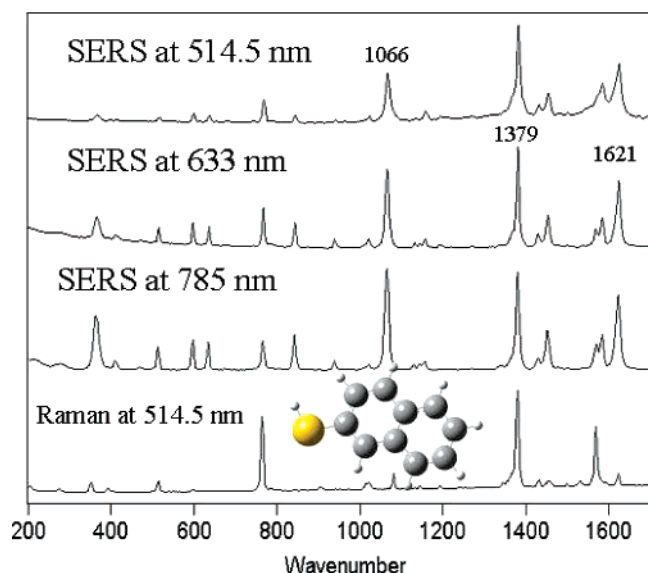


Figure 5. Raman spectra at 514.5 nm and SERS spectra of 2-naphthalenethiol excited with the 514.5, 633, and 785 nm laser lines.

increases slightly from 53.5 to 66.3 nm when the volume of gold added is 20 mL. From this point onward, the size increases faster up to 96 nm when the volume of gold added is 40 mL. This increase in average size could be partly due to aggregation phenomena. However, since ξ is below -20 mV, it is probably related to the growing roughness on the exterior wall of the nanoshells, as it is revealed by the TEM images (Figure 1E,F).

The optical enhancement attained on the fabricated nanostructures was probed using dilute solutions (10^{-5} M) of 2-naphthalenethiol (2-NAT). The 2-NAT analyte was chosen because its vibrational spectra and its SERS

spectra are well-known, since it readily adsorbs onto gold particles.^{31,32} The 2-NAT molecule has an electronic absorption maxima at 242 nm, which is far from the three laser lines used in the present set of experiments: 514.5, 633, and 785 nm, and we have no evidence of surface enhanced resonance Raman scattering (SERS) for the surface complex. The reference Raman spectrum of 2-NAT is therefore the same for all three laser lines and is shown at the bottom of Figure 5. The characteristic SERS spectra of 2-NAT on nanoshells recorded with the 514.5, 633, and 785 nm laser lines can also be seen in Figure 5. The SERS spectrum corresponds to that of 2-NAT chemisorbed onto the metal surface, where the S–H stretching (not shown) is not seen, and in addition, the SERS spectrum on silver sols and gold sols is the same.³³ The SERS results summarized in Figure 6 are for SERS measurements in solution, and although the bimetallic nanoshells cast on glass are great SERS enhancers, for assessment with the original colloidal silver, only the solution results are directly comparable. The three-dimensional plots show the vibrational Raman spectrum in the 300 to 1700 cm^{-1} region (x axis), the variation of the SERS signal intensity (z axis) in colloidal suspensions in kilo counts s^{-1} , and the wavelength of the plasmon absorption (y axis) maxima that correlates with the volume added during the titration as shown in Figure 2A. Figure 6A contains the SERS spectra obtained with the 514 nm laser line, where characteristic vibrational frequencies at 1621, 1379, and 1066 cm^{-1} are highlighted so they can serve as reference for all of the graphs. The enhancement factor (EF) ratio is calculated for a selected vibrational frequency (1379 cm^{-1}), using the SERS intensity of the original colloids and that of the bimetallic structures formed in the same colloidal solution by addition of Au solution and a constant amount of the analyte (2-NAT): $\text{EF} = I_{\text{SERS-AgAu}}/I_{\text{SERS-Ag sols}}$. This ratio was chosen in order to compare the nanoshell

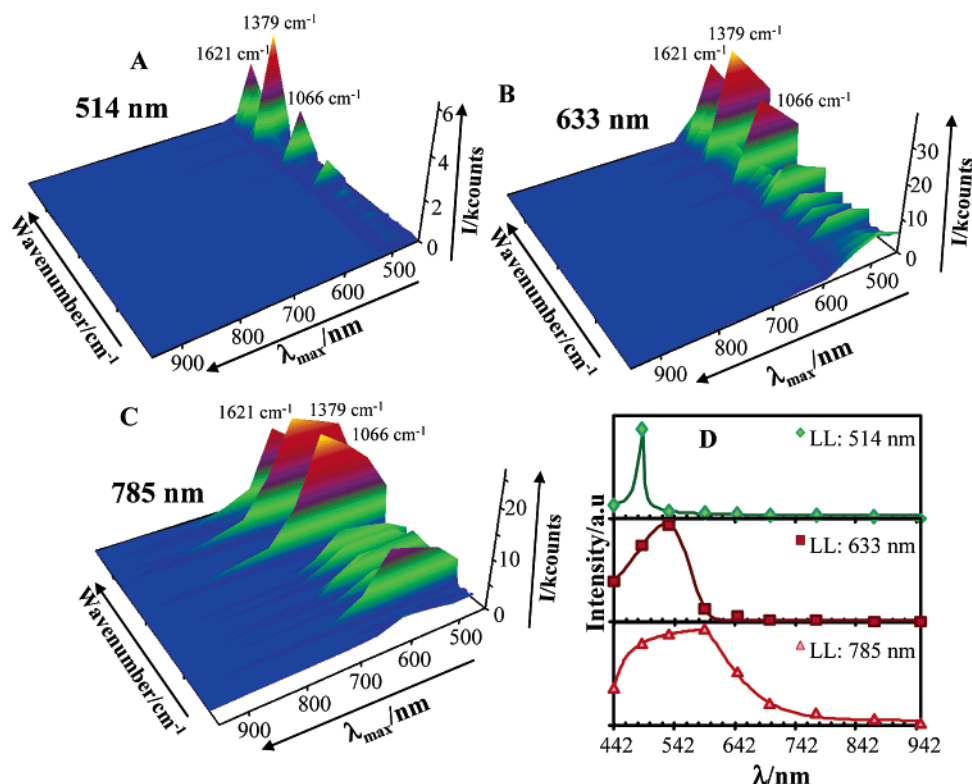


Figure 6. SERS spectra of 2-naphthalenethiol, as a function of the gold added, collected with different excitation laser lines (A) 514, (B) 633, and (C) 785 nm. (D) Variation of the intensity of the band at 1379 cm^{-1} for the three lines, measured under the same experimental conditions.

results to well established silver colloids. For instance, bimetallic nanospheres produced by adding 5 mL of gold to the initial suspension, produce a SERS EF ratio of ca. 7 with respect to the original silver colloids, when excited with the 514.5 laser line. The increment in SERS activity correlates with a shift in the surface plasmon maximum of the new nanoparticles, as compared with silver-citrate colloids, from 442 nm (Ag sols) to 489 nm in the first bimetallic product (Figure 2, second curve from the left, and Figure 1B). The EF ratio decreases rapidly with further addition of the Au solution as can be seen in Figure 6D. Similar SERS results were obtained by exciting with 633 and 785 nm laser lines as shown in Figure 6B,C. A solid plot was selected in these two figures to illustrate the broadening of the SERS activity in terms of the plasmon of the colloidal particles, a property clearly seen in Figure 6D. Figure 6D shows the variation of the intensity of the vibrational band at 1379 cm^{-1} as a function of the ensemble plasmon resonance maximum of the

colloidal solution. For both laser lines, the EF ratio with reference to the regular silver citrate colloids is about 2.5. As can be seen in Figure 6D, the maximum average SERS achieved with the 633 nm laser line is obtained with a solution showing a broad surface plasmon with a maximum at 533 nm. A similar behavior is seen for SERS obtained with the 785 nm laser line where the best SERS activity is observed for the sols with a broad plasmon with a maximum at 593 nm, and the trend of plasmon correlation with excitation frequency is strictly followed. These are average measurements in solution, and further research where the specific hot spot⁹ of isolated bimetallic nanoshells or their aggregates are examined for ultrasensitive analytical applications is underway.

In summary, it is shown that a titration of silver colloids with gold at room-temperature permits the control of the surface plasmon of stable colloidal bimetallic particles. The optical enhancement is demonstrated maximizing the SERS signal of a selected adsorbate. The structures are being tested for ultrasensitive analytical applications of biomolecules.

LA051645L

(31) dos Santos, D. S., Jr.; Alvarez-Puebla, R. A.; Oliveira, O. N., Jr.; Aroca, R. F. *J. Mater. Chem.* **2005**, *15*, 3045–3049.

(32) Alvarez-Puebla, R. A.; dos Santos, D. S., Jr.; Aroca, R. F. *Analyst* **2004**, *129*, 1251–1256.